Biochemistry

 Volume 34, Number 38 September 26, 1995

Articles

Reactive-Site Hydrolyzed *Cucurbita maxima* Trypsin Inhibitor-V: Function, Thermodynamic Stability, and NMR Solution Structure†

Mengli Cai, YuXi Gong, Om Prakash, and Ramaswamy Krishnamoorthi*

Department of Biochemistry, Kansas State University, Manhattan, Kansas 66506

Received June 12, 1995[⊗]

ABSTRACT: Reactive-site (Lys44-Asp45 peptide bond) hydrolyzed *Cucurbita maxima* trypsin inhibitor-V (CMTI-V*) was prepared and characterized: In comparison to the intact form, CMTI-V* exhibited markedly reduced inhibitory properties and binding affinities toward trypsin and human blood coagulation factor XII_a. The equilibrium constant of trypsin-catalyzed hydrolysis, K_{hyd}, defined as [CMTI-V*]/[CMTI-V], was measured to be ~9.4 at 25 °C ($\Delta G° = -1.3$ kcal·mol^{-1}). From the temperature dependence of $\Delta G°$, the following thermodynamic parameters were estimated: $\Delta H° = 1.6$ kcal·mol^{-1} and $\Delta S° = 9.8$ eu. In order to understand the functional and thermodynamic differences between the two forms, the three-dimensional solution structure of CMTI-V* was determined by a combined approach of NMR, distance geometry, and simulated annealing methods. Thus, following sequence-specific and stereospecific resonance assignments, including those of β-, γ-, δ-, and ϵ-hydrogens and valine methyl hydrogens, 809 interhydrogen distances and 123 dihedral angle constraints were determined, resulting in the computation and energy-minimization of 20 structures for CMTI-V*. The average root mean squared deviation in position for equivalent atoms between the 20 individual structures and the mean structure obtained by averaging their coordinates is 0.67 ± 0.15 Å for the main chain atoms and 1.19 ± 0.23 Å for all the non-hydrogen atoms of residues 5−40 and residues 48−67. Comparison of the mean structure of CMTI-V* with the average NMR solution structure of CMTI-V [Cai, M., Gong, Y., Kao, J. K.-F., and Krishnamoorthi, R. (1995) *Biochemistry 34*, 5201−5211] indicated tertiary structural changes in the binding loop and N-terminal regions; all the secondary structural elements were preserved. The newly formed termini in CMTI-V* are separated apart and more flexible. Structural differences were reflected in the chemical shifts of the backbone hydrogen atoms and the pK_a of His11 side chain, which changed from 5.58 ± 0.02 in the intact form to 5.81 ± 0.02 in the hydrolyzed form; the change in pK_a is likely due to a stronger hydrogen bond, as reflected by a shorter distance between $N^{\delta}H$ of His11 and main-chain oxygen of Pro10. The reduced binding affinities for trypsin and factor XII_a and increased entropy of CMTI-V* are consistent with the increased flexibility of the cleaved binding loop.

Serine proteinase inhibitors present an ideal system for studying structure−function relationships and their modulation by protein−protein interactions: Like substrates, they form 1:1 complexes with their cognate enzymes, but their reactive-site peptide bonds are hydrolyzed at a much slower rate with the formation of modified or clipped inhibitors,

† This work has been supported by a grant from the National Institutes of Health (HL-40789 to R.K.). R.K. is an NIH Research Career Development Awardee (1994−1999). The 11.75 T NMR instrument used for this project was purchased with funds from an NSF-EPSCoR grant. This is contribution 96-36-J from the Kansas Agricultural Experiment Station.

* Author to whom correspondence should be addressed. E-mail: krish@ksuvm.ksu.edu. Phone: (913) 532-6262. Fax: (913) 532-7278.

⊗ Abstract published in *Advance ACS Abstracts*, September 1, 1995.

0006-2960/95/0434-12087$09.00/0

which are also generally inhibitors.

According to the standard mechanism (Laskowski and Kato, 1980), the hydrolysis reaction can be written as follows

$$E + I \rightleftarrows C \rightleftarrows E + I^*$$

where E is the enzyme and C is the stable complex between enzyme and inhibitor and I and I* are the intact and hydrolyzed inhibitor, respectively. The equilibrium constant of hydrolysis, K_{hyd}, is defined as

$$K_{hyd} = [I^*]/[I]$$

Thus, in principle, it is possible to determine functional properties, including binding affinities, thermodynamics of the hydrolysis reaction, and finally, three-dimensional structures of the two forms of a given inhibitor. With structures of both forms of a given inhibitor in hand, intramolecular interactions that influence its functional and thermodynamic properties may be identified. Dynamics also play a crucial role in the functioning of a protein (Karplus, 1986).

Such an approach has been recognized and utilized by earlier researchers in the field. Intact and reactive-site hydrolyzed forms of ovomucoid third domains, which inhibit chymotrypsin, subtilisin, and elastase, and which are members of the Kazal family of inhibitors (Laskowski & Kato, 1980), have been extensively studied by X-ray crystallography (Weber et al., 1981; Papamokos et al., 1982; Fujinaga et al., 1987; Musil et al., 1991) and nuclear magnetic resonance (NMR) (Krezel et al., 1994; Walkenhorst et al., 1994) methods. Hydrolysis equilibrium constants have also been determined for a number of naturally occurring ovomucoid third domains, and on the basis of the available X-ray crystal and NMR solution structures of both intact and hydrolyzed forms, the structural basis has been explored to account for the values of K_{hyd} measured (Musil et al., 1991; Ardelt et al., 1991). K_{hyd} values have also been measured for a few members of the squash family of inhibitors (Krishnamoorthi et al., 1992; Otlewski and Zybryt, 1994). Identification of perturbed side-chain−side-chain interactions is important in the rational designing of more effective inhibitors. This has ramifications in the making of molecules of therapeutic importance, as serine proteinase inhibitors control the activities of proteolytic enzymes involved in various biological processes, including blood-clotting (Neurath, 1984). X-ray crystal structures have been determined for a number of serine proteinase inhibitors; a sizable number of NMR solution structures has also become available in recent years (Bode and Huber, 1992).

We have extended the approach described above to *Cucurbita maxima* trypsin inhibitor-V (CMTI-V;[1] M_r ~7 Kda), a member of the potato I inhibitor family. CMTI-V is also a specific inhibitor of human blood coagulation factor XII_a. It has 68 amino acid residues, including a Cys3−Cys48 disulfide bridge. The reactive site has been established to be the peptide bond between Lys44 and Asp45 (Krishnamoorthi et al., 1990). CMTI-V is unique in that among its family members of known three-dimensional structures, it alone has a cystine bridge. Recently, we reported the three-dimensional solution structure of CMTI-V (Cai et al., 1995a). Other members of the Potato I inhibitor family that have been extensively studied are chymotrypsin inhibitor-2 (CI-2) from barley and eglin c from the leech *Hirudo medicinalis*: the three-dimensional structures of CI-2 in the solid (McPhalen and James, 1988) and solution phases (Clore et al., 1987a,b) have been determined. Similarly, both crystal (Hipler et al., 1992) and solution (Hyberts et al., 1992) phase three-dimensional structures of eglin c are known. In addition, a low-resolution X-ray crystal structure has been recently reported for reactive-site hydrolyzed eglin c (Betzel et al., 1993). On the basis of heteronuclear relaxation and NOE measurements, backbone dynamics of CI-2 (Shaw et al., 1995) and eglin c (Peng and Wagner, 1992) have been reported.

Only a very few comparative studies of structures and dynamics of intact and reactive-site hydrolyzed inhibitors under identical conditions have been reported to date: turkey ovomucoid third domain is the first serine proteinase inhibitor for which a comparison of three-dimensional solution structures of the intact and hydrolyzed forms has been recently reported (Krezel et al., 1994; Walkenhorst et al., 1994). Earlier, we described a comparative NMR study of intact and reactive-site hydrolyzed *Cucurbita maxima* trypsin inhibitor-III (CMTI-III; M_r ~3 Kd)—a member of the squash inhibitor family (Wieczorek et al., 1985)—and noted conservation of the secondary structure, but perturbation of the tertiary structure, between the two forms (Krishnamoorthi et al., 1992). Perkins et al. (1992) have characterized by NMR and Fourier transform infrared spectroscopy the secondary structural changes that stabilize reactive-site cleaved SERPINs.

Herein we report on a comparison of the functional and thermodynamic properties of intact and hydrolyzed forms of CMTI-V. We also present the NMR-determined three-dimensional solution structure of CMTI-V* and compare it to that of CMTI-V under identical conditions (Cai et al., 1995a) in order to identify the structural basis of the observed differences.

MATERIALS AND METHODS

Proteins. Pure CMTI-V was isolated from pumpkin seeds, as previously described (Krishnamoorthi et al., 1990). CMTI-V* was obtained by reacting CMTI-V with ~5% by mole of trypsin, followed by purification by reversed-phase high-pressure liquid chromatography (HPLC). A typical NMR sample was prepared by dissolving ~20 mg of the protein in 0.5 mL of H_2O or D_2O, containing 0.2 M KCl. The pH of the protein solution was adjusted with 0.2 M NaOD and/or 0.2 M DCl, using an Ingold microcombination glass electrode on a Fisher 815 MP pH meter.

NMR Spectroscopy. DQ-COSY (Rance *et al.*, 1983), TOCSY (Bax & Davis, 1985), NOESY (Anil Kumar *et al.*, 1980), and PE-COSY (Mueller, 1987) experiments were carried out on a 11.75 T (500 MHz for ^1H) Varian Unity*plus* NMR instrument. All experiments were carried out at 10,

[1] Abbreviations: CMTI-V, *Cucurbita maxima* trypsin inhibitor-V; CMTI-V*, reactive-site hydrolyzed *Cucurbita maxima* trypsin inhibitor-V; NMR, nuclear magnetic resonance; NOE, nuclear Overhauser effect; CI-2, chymotrypsin inhibitor-2; DQF-COSY, double-quantum-filtered correlated spectroscopy; P.E. COSY, primitive extended correlated spectroscopy; TOCSY, total correlated spectroscopy; NOESY, nuclear Overhauser effect spectroscopy; RMSD, root mean squared deviation; ppm, parts per million.

[2] Atomic coordinates for the refined average structure of CMTI-V*, along with the NMR constraints, have been deposited with Protein Data Bank, Brookhaven National Laboratories, Long Island, NY 11973, under the accession code 1HYM.

30, and 50 °C to resolve the N*HC*$^{\alpha}$*H* cross-peaks that overlapped with the water signal. Data collection and processing procedures were used as described before (Cai et al., 1995a). Residues whose amide hydrogen cross peaks persisted 24 h or more after dissolution of the protein in D_2O were considered to be hydrogen-bonded, as was done in the case of CMTI-V (Cai et al., 1995a).

Assay of Trypsin and Factor XII$_a$ Inhibitory Activities. The inhibitory activities of CMTI-V and CMTI-V* were determined by measuring the residual activity of trypsin or factor XII_a after adding varying amounts of the inhibitor: For trypsin activity assay, increasing amounts of CMTI-V or CMTI-V* were mixed with a fixed amount of trypsin (Sigma, ~2.76 μg) in a 1 mL reaction buffer containing 0.5 M Tris−HCl and 0.02 M $CaCl_2$, pH 8.2. The mixture was incubated at room temperature for 5 min. Activity of the free enzyme was assayed by adding 30 μL of the substrate, N_{α}-benzoyl-DL-arginine-*p*-nitroanilide hydrocloride (BAPNA; 10 mg/mL in dimethyl sulfoxide). For factor XII_a activity assay, various amounts of CMTI-V or CMTI-V* were mixed with a fixed amount of β-factor XII_a (Calbiochem, ~5 μg) in 1 mL of reaction buffer, containing 0.05 M Tris−HCl, 20 μL of bovine serum albumin (2 mg/mL), pH 8.2. The mixture was incubated at room temperature for 5 min. Activity of free β-factor XII_a was determined by adding 20 μL of the substrate, D-prolyl-L-phenyalanyl-L-arginine-*p*-nitroanilide (S-2302, 5.75 mg/mL in water). In each case, activity of the free enzyme was determined by monitoring the absorbance of the released *p*-nitroanilide at 405 nm on a Hitachi U-2000 UV−vis spectrophotometer. Protease and inhibitor concentrations were determined by using the Pierce micro BCA protein assay reagent.

Determination of Enzyme:Inhibitor Complex Dissociation Constants (K_i). Dissociation constants of trypsin:CMTI-V, trypsin:CMTI-V*, factor XII_a:CMTI-V, and factor XII_a:CMTI-V* complexes were each determined by means Lineweaver−Burk plots (double reciprocal plot of the Michaelis-Menten equation; Stryer, 1988). The slope ratio of the plots with and without inhibitor was used to calculate K_i. For trypsin:CMTI-V (or CMTI-V*) complex, a double reciprocal plot was generated by reacting ~4 μg of trypsin and $1.4-8.2 \times 10^{-4}$ M BAPNA with no inhibitor present in 1 mL buffer, containing 0.5 M Tris−HCl and 20 mM $CaCl_2$ at pH 8.2, and another plot under identical conditions, but trypsin was preincubated with 4.8×10^{-8} M CMTI-V (or 9.8×10^{-8} M CMTI-V*) for 5 min before BAPNA was added. The hydrolysis rate was determined by following the absorbance increase at 405 nm. For factor XII_a:CMTI-V (or CMTI-V*) complex, the same approach was used, except that the reacting buffer was 0.05 M Tris−HCl at pH 8.0 and $(0.93-9.3) \times 10^{-5}$ M S-2302 and ~9 μg of factor XII_a were used as substrate and enzyme. The concentrations of inhibitors were 2.42×10^{-8} M for CMTI-V and 5.9×10^{-8} M for CMTI-V*.

K_{hyd} Determination. About 2 mg of lyophilized CMTI-V or CMTI-V* was dissolved in 0.5 mL water, containing 50 mM potassium phosphate buffer at pH 6.75. A catalytic amount of trypsin (10 μL of ~0.5 mM stock solution; ~1 mol %) was added to the inhibitor solution. The concentration of trypsin was estimated according to its molecular mass (M_r 24 kDa). The reaction mixture was incubated in an appropriate temperature bath. Samples (~50 μL) were withdrawn periodically, and CMTI-V and CMTI-V* were separated by reversed-phase HPLC (Krishnamoorthi et al., 1990). The corresponding peak areas were measured by means of Varian chromatography software, and their ratios were used for the relative concentrations of the two forms. K_{hyd} values were obtained when no change in the ratios was noticed with time. The same equilibrium position was reached starting either with CMTI-V or with CMTI-V* at 25 °C. At other temperatures (4, 15, 37, and 45 °C), the equilibration was followed only with CMTI-V, and the hydrolysis constant was determined when no change in the relative peak areas was noticed with time.

NMR Solution Structure Determination. The procedure described previously for the structure determination of CMTI-V (Cai et al., 1995a) was followed. Thus, backbone torsional angles, ϕ, were determined from $^3J_{N\alpha}$ coupling constants (Driscoll et al., 1989; Cai et al., 1992; Clubb et al., 1994), and χ_i torsional angles were estimated from stereospecific assignments of methylene hydrogens and methyl groups (Wagner et al., 1987; Cai et al., 1995b,c). All six prolines in the protein were identified to be *trans* in conformation. Pro4, Pro29, Pro41, Pro64, and Pro65 were found to have the *Up* pucker and Pro10 the *Down* pucker, as in CMTI-V (Cai et al., 1995d).

By use of the criteria described previously for the conversion of NOESY cross peak intensities into distance constraints (Cai et al., 1995a), a total of 809 interproton distance constraints were determined, which included 333 intraresidue, 188 sequential (for residues i and j, $j - i = 1$), 74 short range ($j - i < 5$), 168 long range ($j - i \geq 5$), and 46 constraints on the basis of 23 hydrogen bonds. These constraints, along with 123 dihedral angle constraints, were used for structure computation, using the simulated annealing (SA) protocol (Brünger, 1992; Nilges et al., 1988), as described previously (Cai et al., 1995a). A mean structure, designated ⟨SA⟩, was obtained by best-fitting the 20 best SA structures to each other, averaging their coordinates, and refining the resulting structure by energy minimization with the SA method (Driscoll et al., 1989). The refined mean structure, together with the NMR constraints, has been deposited with the Brookhaven Protein Data Bank (accession code 1HYM).

RESULTS

Comparison of Inhibitory Activities and Binding Affinities of Intact and Cleaved CMTI-V toward Trypsin and Factor XII$_a$. The inhibitory activities of CMTI-V and CMTI-V* toward trypsin are compared in Figure 1A and toward factor XII_a in Figure 1B. The hydrolyzed inhibitor is less effective toward either of the enzymes. For 50% inhibition of either trypsin or factor XII_a activity, about 5-fold increase of CMTI-V* is required, relative to CMTI-V. The competitive nature of the weak inhibition exhibited by CMTI-V* was established from the double-reciprocal plots shown for the trypsin−BAPNA reaction with and without CMTI-V or CMTI-V* in Figure 2A, and for the factor XII_a-S2302 reaction with and without the intact or modified inhibitor in Figure 2B. In each case, the straight lines with and without inhibitor have different slope values but the same intercept values. The enzyme:inhibitor complex dissociation constants, K_i, were calculated from the slope ratios. Thus, the following values were obtained: 5.5×10^{-8} M and 3.3×10^{-7} M for trypsin:CMTI-V and trypsin:CMTI-V* complexes, respectively, and

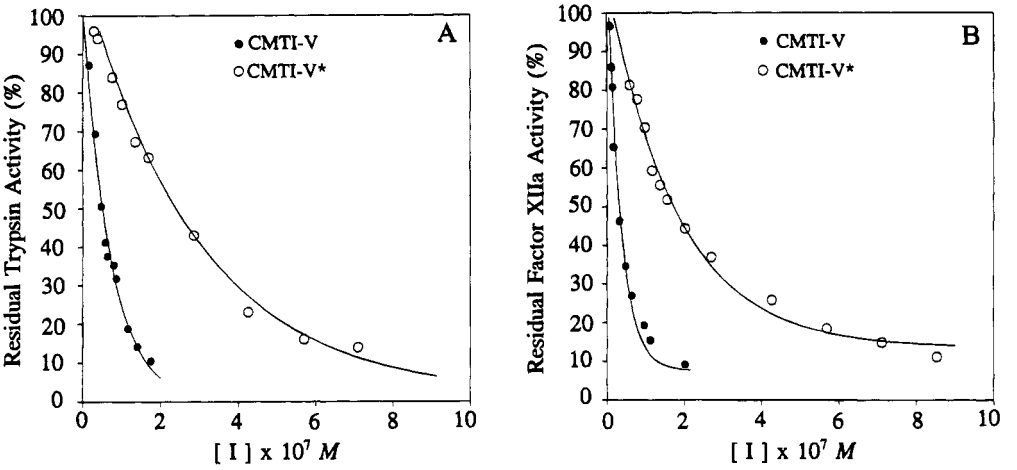

FIGURE 1: (A) Inhibition of trypsin by varying amounts of CMTI-V and CMTI-V*. (B) Inhibition of human factor XII_a by varying amounts of CMTI-V and CMTI-V*. The curved lines are computer-generated best fits to the data points; these have no theoretical significance, and are meant to guide the eye.

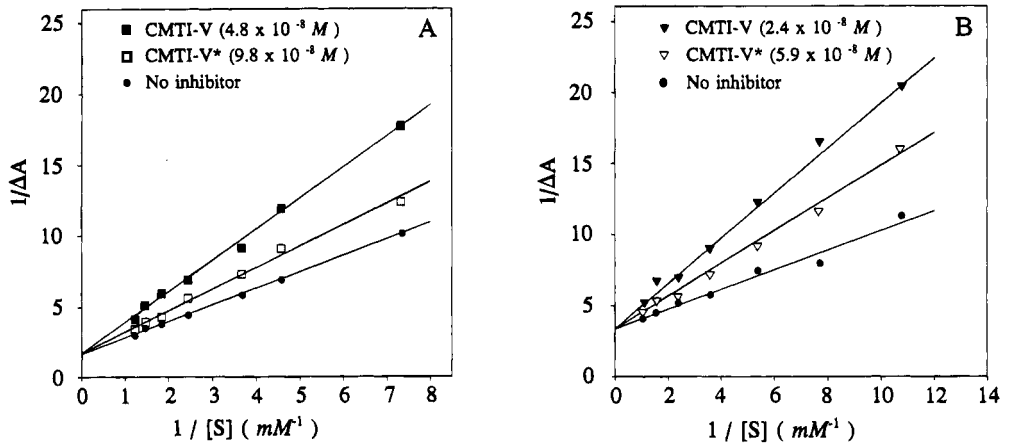

FIGURE 2: Lineweaver–Burk plots of inhibition by CMTI-V and CMTI-V* of (A) trypsin and (B) human factor XII_a.

1.9×10^{-8} M and 0.8×10^{-7} M for factor XII_a:CMTI-V and factor XII_a:CMTI-V* complexes, respectively. These data demonstrate that the binding affinities of the modified inhibitor toward both trypsin and factor XIIa are significantly reduced.

Thermodynamics of the Equilibrium between Intact and Hydrolyzed CMTI-V. Figure 3 shows an HPLC trace of the equilibrium mixture of intact and hydrolyzed CMTI-V, catalyzed by trypsin at 25 °C. The hydrolyzed form predominates, yielding a K_{hyd} value of about 9.4 ($\Delta G° = -1.3$ kcal·mol^{-1}). In order to identify the relative contributions of enthalpy and entropy changes to the standard free energy change, the temperature dependence of the equilibrium constant was determined over the range 4–45 °C. A linear plot of $\Delta G°$ as a function of temperature was drawn (Figure 4), and the following parameters were estimated from the intercept and slope, respectively: $\Delta H° = 1.6$ kcal·mol^{-1} and $\Delta S° = 9.8$ eu. Because of the errors associated with the measurements of small areas of HPLC peaks corresponding to the intact form, we use these parameters for qualitative interpretations only. Thus, it is clear that although the hydrolysis reaction is endothermic—i.e., CMTI-V* is less stable compared to CMTI-V—the equilibrium is entropy-driven.

NMR Structural Studies. Sequential and stereospecific proton resonance assignments of CMTI-V*, made according to standard 2D NMR procedures (Wüthrich, 1986), are

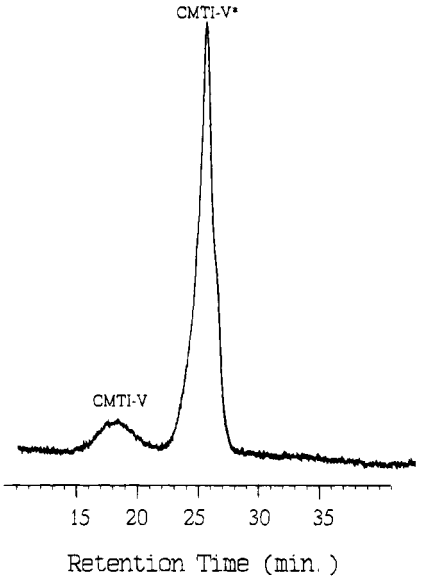

FIGURE 3: HPLC trace of an equilibrium mixture at 25 °C of intact and reactive-site hydrolyzed CMTI-V in the presence of a catalytic amount of trypsin.

provided as supporting information. Statistical details for the best 20 SA structures and the refined mean structure are given in Table 1. Superposition of the main chain atoms (C, C^{α}, and N atoms) for the 20 SA structures is shown in

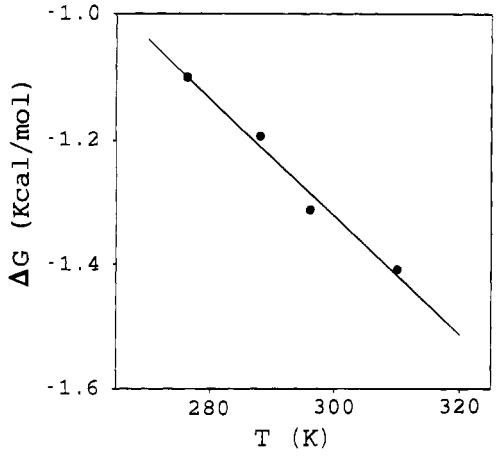

FIGURE 4: Temperature dependence of the CMTI-V ⇄ CMTI-V* equilibrium. $\Delta H°$ and $\Delta S°$ were estimated from the intercept and slope, respectively.

Figure 5. The conformation of all main chain atoms for the 20 SA structures is well-conserved, except for the first few N-terminal residues and the last C-terminal residue. A loop region from residues 40−47 displays a higher RMSD, compared to other regions. The solution structure of CMTI-V* retains the rigid scaffold region and the flexible loop region, which were characterized in CMTI-V (Cai et al., 1995a) and which are common to serine proteinase inhibitors in general (Bode & Huber, 1992). The rigid body region preserves the major α-helix (residues 18−28) and three pairs of β-sheets (residues 8−9 and 62−60 anti-parallel to residues 67−66 and 54−56, respectively, and residues 32−37 parallel to 51−55), connected by the cleaved reactive-site loop and four turns (type II, 12−15; type I, 28−31 and 47−50; and type III, 56−59).

DISCUSSION

The significant reduction in inhibitory activities and binding affinities toward both trypsin and factor XII_a and thermodynamic properties—equilibrium in favor of the hydrolyzed form and driven by gain in entropy—of CMTI-V* may be explained reasonably on a structural basis by comparing the average NMR solution structures of intact (Cai et al., 1995a) and hydrolyzed CMTI-V: Figure 6 depicts the best-fit superposition of average refined structures of CMTI-V and CMTI-V*; the overall global folding and major secondary structural elements are conserved in the hydrolyzed inhibitor. The average RMSD of backbone atoms between the refined average structures of CMTI-V and CMTI-V* for residues 5−38 and residues 48−68 is only 0.88 Å (Figure 7). Differences are, however, observed in the binding loop region and the N-terminal segment.

Binding Loop Region. The region of CMTI-V* that displays the biggest difference from CMTI-V is the binding loop, as evidenced by the RMSD values given in Figure 7. This is also reflected by the differences in chemical shifts of the $C^{\alpha}H$ and NH atoms noted between the intact and modified inhibitor (Figure 8). The RMSD of the 20 SA structures from their mean structure in the binding loop region is much higher in CMTI-V* (4.5 Å for main chain atoms) than that in CMTI-V (2.7 Å; Cai et al., 1995a). This result suggests an increase in the flexibility of the binding loop region upon hydrolysis of the reactive-site Lys44-Asp45 peptide bond. NMR studies of backbone dynamics of CI-2 (Shaw et al., 1995) have also indicated an increase in the flexibility of the hydrolyzed form at the reactive-site region. However, the two newly formed terminii do not appear to be freely mobile in the solution like a random coil, as indicated by the fact that the chemical shifts of the binding loop residues are different from the random coil values (Wüthrich, 1986). Furthermore, as found in CMTI-V (Cai et al., 1995a,c) both Arg50 and Arg52 possess the same rigid conformations, as all the methylene hydrogens could be

Table 1: Structure Statistics for CMTI-V*

Distance Constraints			
		rms deviations from exptl distance constraints (Å)	
total	distance	SA[a]	⟨SA⟩$_r$[b]
809	all	0.0078 ± 0.0004	0.0065
333	intraresidue	0.0043 ± 0.0011	0.0056
188	sequential ($\|i-j\|=1$)	0.0115 ± 0.0065	0.0104
74	short range ($\|i-j\| \leq 5$)	0.0033 ± 0.0033	0.0000
168	long range ($\|i-j\| > 5$)	0.0055 ± 0.0055	0.0038
46	H-bond	0.0091 ± 0.0042	0.0028

Torsional Angle Constraints			
		rms deviations from exptl distance constraints (deg)	
total	angle	SA[a]	⟨SA⟩$_r$[b]
123	all	0.226 ± 0.027	0.222
54	ϕ angles	0.048 ± 0.048	0.001
69	χ angles	0.294 ± 0.032	0.296

Energies[c] (kcal/mol)		
	SA[a]	⟨SA⟩$_r$[b]
F_{noe}	2.58 ± 2.02	1.68
F_{tor}	0.97 ± 0.12	0.94
F_{repel}	3.35 ± 0.32	2.65
F_{L-J}	−337 ± 7	−338

RMS Deviations from Idealized Geometry		
	SA[a]	⟨SA⟩$_r$[b]
bond (Å)	0.0076 ± 0.0007	0.0074
angle (deg)	2.1248 ± 0.1374	2.0872
impropers (deg)	0.1021 ± 0.0506	0.0663

RMS Deviations of 20 SA's and Their Mean Structure (Å)	
whole protein	
main chain	2.00 ± 0.72
all heavy atoms	2.42 ± 0.67
residues 3−40 and residue 49−67	
main chain	0.67 ± 0.15
all heavy atoms	1.19 ± 0.23
loop regeon (residue 41−48)	
main chain	4.49 ± 2.19
all heavy atoms	5.30 ± 2.03

[a] SA represents the 20 individual structures refined by the simulated annealing method and ⟨SA⟩$_r$ represents the refined mean structure, as described in the text. [b] Root mean squared deviations in angstroms when the calculated final distance between hydrogens in the structure after simulated annealing refinements exceeds the boundaries of distance constraints and torsional angle constraints, averaged over all constraints of different constraints groups listed in the table. [c] The force constants used for these calculations are 50 kcal/(mol Å^2) for distance constraints, 500 kcal/(mol rad^2) for torsional angle constraints, and 4 kcal/(mol Å^2) for the repulsion term. F_{noe}, F_{tor}, and F_{repel} are, respectively, the constraint violation energies associated with distance constraints and torsional angle constraints and the van der Waals repulsion energy with hard-sphere van der Waals radii set to 0.8 times the standard values used in the CHARMm empirical energy function (Brooks et al., 1983). E_{L-J} is the van der Waals energy recalculated with the same coordinates, but with the electrostatic terms included.

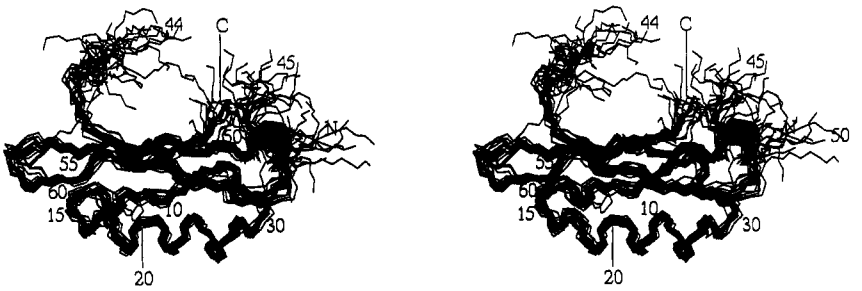

FIGURE 5: Stereoview of the best-fit superposition of the 20 SA structures of CMTI-V*. The main chain atoms (N, C^{α}, and $C^{C=O}$), including the Cys3−Cys48 disulfide bridge, are shown.

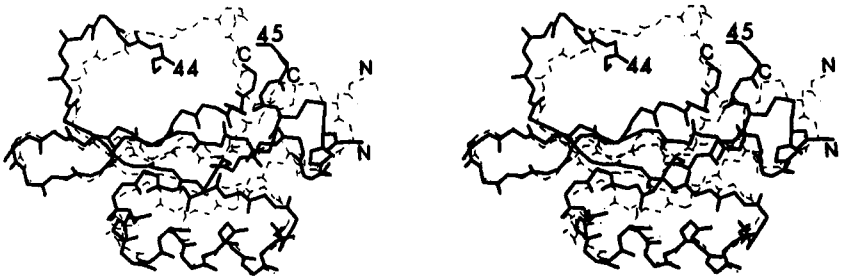

FIGURE 6: Stereoview of superposition of refined average solution structures of CMTI-V (broken thin line; Cai et al., 1995a) and CMTI-V* (solid thick line). Main chain atoms and the Cys3−Cys48 bridge only are drawn.

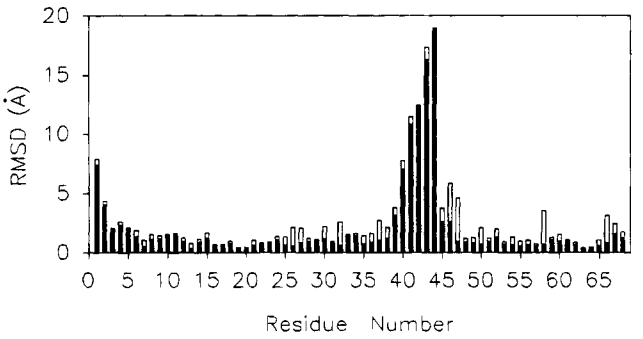

FIGURE 7: RMSD between the refined average structures of CMTI-V and CMTI-V* as a function of residue number. Open bars correspond to all heavy atoms, and filled bars correspond to main chain atoms only.

stereospecifically assigned and $\chi_1-\chi_4$ torsional angles determined. The rigid conformations of these two charged side chains in CMTI-V* suggest that the hydrogen bonding interactions between Arg52 and Thr43 and between Arg50 and Asp45 (Cai et al., 1995a) are maintained in the reactive-site hydrolyzed form.

N-Terminal Segment. The N-terminal segment of CMTI-V* shows significant perturbations in comparison to that of CMTI-V, as suggested by the slightly higher RMSD between the two forms of the inhibitor (Figure 7), the small differences in the chemical shifts of the backbone atoms in this region (Figure 8), and the pH titration profile of His11 side chain in the two forms (Figure 9). From the pH-dependence of the chemical shift of $C^{\epsilon}H$ of His11, a pK_a of 5.81 ± 0.02 was measured for CMTI-V* and a value of 5.58 ± 0.02 for CMTI-V. An inspection of the average solution structures of both forms reveals that the distance from N^{δ} of His11 to the main-chain oxygen of Pro10 is shorter in CMTI-V* (3.28 Å) as compared to that (3.71 Å) in CMTI-V. This observation suggests a stronger hydrogen bond between the ring NH of His11 and the main-chain oxygen of Pro10 in CMTI-V* than that in CMTI-V, thus making the ring NH harder to ionize in CMTI-V*. Strong NH−NH NOEs between His11

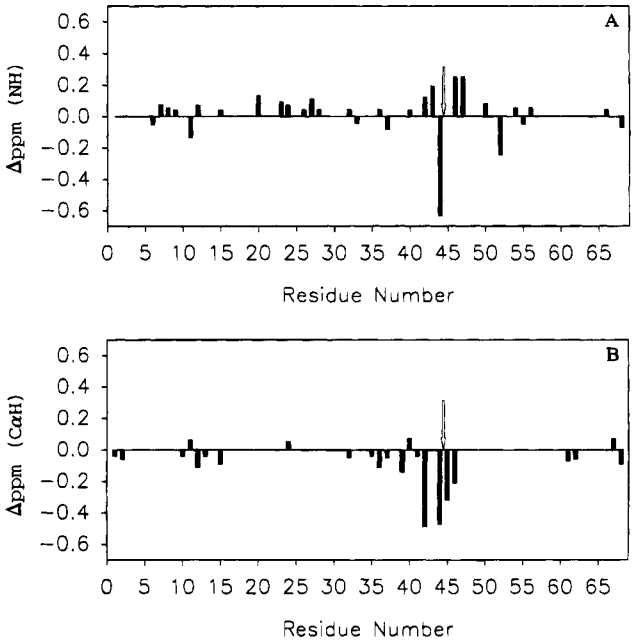

FIGURE 8: (A) Backbone amide hydrogen chemical shift differences between CMTI-V* and CMTI-V (Δppm = CMTI-V* − CMTI-V) as a function of residue number. (B) $C^{\alpha}H$ chemical shift differences between CMTI-V* and CMTI-V (Δppm = CMTI-V* − CMTI-V) as a function of residue number. For the purpose of clarity, values equal to or greater than the error limit of ± 0.03 ppm alone are shown. The vertical arrow in each case indicates the location of the reactive site.

and Leu12 and between Leu12 and Val13 observed in the hydrolyzed form, but not in the intact form, are another indication of the conformational change taking place in the N-terminal segment. In the calculated average solution structures, ϕ and ψ angles of Gly5 (130 and 161, respectively, in CMTI-V, −159 and −134, respectively, in CMTI-V*) and His11 (−120 and 75, respectively, in CMTI-V, and −90 and 92, respectively, in CMTI-V*) and the ϕ angle of Lys6 (−44 in CMTI-V and −90 in CMTI-V*) indicate noticeable differences between the intact and modified forms

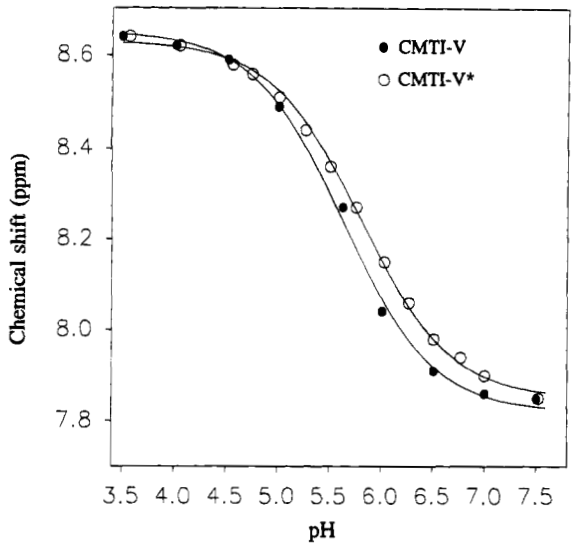

FIGURE 9: pH titration of His11 $C^{\epsilon}H$ in CMTI-V* and CMTI-V. The lines drawn through the points represent the best fits to the Henderson–Hasselbach equation for a single proton dissociation. pK_a values of 5.81 and 5.53 (±0.02) were obtained for CMTI-V* and CMTI-V, respectively.

of the inhibitor. The N-terminal segment, as it is connected to the binding loop through a disulfide bond (Cys3–Cys48), moves together with the binding loop, and thus shows a higher displacement.

Trp9. On the basis of the pattern of observed NOESY cross-peaks, Trp9 is found to retain its conformation in CMTI-V*. There is a strong indication of the preservation of the hydrogen bond between Trp9 and Ile23 that holds the N-terminal segment and the α-helix together, as the average distances from Trp9 N^{ϵ} and $N^{\epsilon}H$ to the backbone oxygen of Ile23 are 3.85 ± 0.40 Å and 3.00 ± 0.15 Å, respectively—values similar to those found in CMTI-V (Cai et al., 1995a). However, Trp9 appears to be more flexible in the cleaved inhibitor: The average RMSD of all its heavy atoms is 0.50 ± 0.30 Å in CMTI-V*, whereas it is 0.29 ± 0.11 Å in CMTI-V. The gain in Trp9 side-chain flexibility in CMTI-V* is probably due to the more flexible N-terminal segment, as discussed above. Trp9 also displays high RMSD between the two forms of inhibitor (1.6 Å for all heavy atoms). This suggests a conformational difference for Trp9 in CMTI-V and CMTI-V*. NOEs from Trp9 side-chain hydrogens to Pro65 side-chain hydrogens, which were identified in CMTI-V, are missing in CMTI-V*. Pro65 conformation is retained in CMTI-V*, as indicated by its superposition over that in the CMTI-V inhibitor with an RMSD of only 0.47 Å for all heavy atoms.

α-Helix and β-Sheets. The α-helix and β-sheet segments are well conserved between intact and hydrolyzed CMTI-V, as indicated by the low average RMSD values (Figure 7) and small chemical shift differences for the backbone atoms between the two forms of the inhibitor (Figure 8). The chemical shift differences may arise out of changes in the Trp9 ring current shifts caused by structural changes in the N-terminal segment. As in CMTI-V (Cai et al., 1995a), the side chains of Lys6 and Lys21 adopt rigid conformations and retain hydrogen-bonding interactions with Gln27 and Ala33, respectively, in the hydrolyzed inhibitor. Amide hydrogens of Asp38 and Ile67 in CMTI-V were considered to be hydrogen-bonded to the other strand of the β-sheet (Cai et al., 1995a). These two amide hydrogens in CMTI-V*, however, exchanged with D_2O within 24 h of dissolution of the protein in D_2O. The hydrogen bonds formed from these two amide hydrogens, however, appear not to be broken, based on the following: Noticeable chemical shift differences were not observed for these two hydrogens (Figure 8), as otherwise would be the case. Secondly, long range NOEs between two strands of the β-sheet remain the same in CMTI-V* as in CMTI-V, which indicates that the β-sheet structure elements remain the same in both forms of the inhibitor. The observed differences in the exchange rates may be attributed to differences in solvent accessibility of these two residues.

CONCLUSIONS

The data presented here appear to provide a coherent picture of the interplay between structure, stability, and function in the case of CMTI-V. Determination of thermodynamic quantities and functional properties of intact and reactive-site hydrolyzed CMTI-V indicate that CMTI-V* has gained entropy, with a concomitant loss in inhibitory function and binding affinity toward its cognate enzymes. The NMR structural investigation supports the above notion in that the binding loop and the N-terminal segment have become significantly more flexible in the hydrolyzed inhibitor, despite preservation of the secondary structural elements in both forms of the protein. It is of interest to compare qualitatively the thermodynamic quantities measured for the hydrolysis equilibrium of CMTI-V with those reported for CMTI-III, a squash family inhibitor (Krishnamoorthi et al., 1992): whereas CMTI-III* is energetically more stable ($\Delta H°$ −ve) and less favored by entropy ($\Delta S°$ has a negative value) than CMTI-III, CMTI-V* is less stable, but more favored by entropy than CMTI-V (both $\Delta H°$ and $\Delta S°$ +ve). In other words, the driving force for the hydrolysis equilibrium is increased stability in the case of CMTI-III* and entropy gain in the case of CMTI-V*. A recombinant version of CMTI-V has been produced (Wen et al., 1993), and efforts are underway to produce mutants that would display significantly altered K_{hyd}. Such mutants will be structurally characterized in order to identify intramolecular forces that modulate inhibitor stability and functional efficacy.

ACKNOWLEDGMENT

The authors thank Dr. Jianhua Liu and Mr. Dave Manning for their technical assistance.

SUPPORTING INFORMATION AVAILABLE

One table of ^1H NMR chemical shifts of CMTI-V* (5 pages). Ordering information is given on any current masthead page.

REFERENCES

Anil Kumar, Ernst, R. R., & Wüthrich, K. (1990) *Biochem. Biophys. Res. Commun. 95*, 1–6.

Ardelt, W., & Laskowski, M., Jr. (1991) *J. Mol. Biol. 220*, 1041–1053.

Bax, A., & Davis, D. G. (1985) *J. Magn. Reson. 65*, 355–360.

Betzel, C., Dauter, Z., Genov, N., Lamzin, V., Navaza, J., Schnebli, H. P., Visanji, M., & Wilson, K. S. (1993) *FEBS Lett. 317*, 185–188.

Bode, W., & Huber, R. (1992) *Eur. J. Biochem. 204*, 433–451.

Brooks, B. R., Bruccoleri, R. E., Olafson, R. E., States, D. J., Swaminathan, S., & Karplus, M. (1983) *J. Comput. Chem. 4*, 187−217.

Brünger, A. T. (1992) X-PLOR version 3.1, Yale University Press, New Haven and London.

Cai, M., Bradford, E. G., & Timkovich, R. (1992) *Biochemistry 31*, 8603−8612.

Cai, M., Gong, Y., Kao, J.-L., & Krishnamoorthi, R. (1995a) *Biochemistry 34*, 5201−5211.

Cai, M., Liu, J., Gong, Y., & Krishnamoorthi, R. (1995b) *J. Magn. Reson., Ser. B 107*, 172−178.

Cai, M., Gong, Y., & Krishnamoorthi, R. (1995c) *J. Magn. Reson., Ser. B 106*, 297−299.

Cai, M., Huang, Y., Liu, J., & Krishnamoorthi, R. (1995d) *J. Biomol. NMR*, in press.

Clore, G. M., Gronenborn, A. M., James, M. N. G., Kjaer, M., McPhalen, C. A., & Poulsen, F. M. (1987a) *Protein Eng. 1*, 313−318.

Clore, G. M., Gronenborn, A. M., Kjaer, M., & Poulsen, F. M. (1987b) *Protein Eng. 1*, 305−311.

Clubb, R. T., Ferguson, S. B., Walsh, C. T., & Wagner, G. (1994) *Biochemistry 33*, 2761−2772.

Driscoll, P. C., Gronenborn, A. M., Beress, L., & Clore, G. M. (1989) *Biochemistry 28*, 2188−2198.

Fujinaga, M., Sielecki, A. R., Read, R. J., Ardelt, W., Laskowski, M., Jr., & James, M. N. G. (1987) *J. Mol. Biol. 195*, 397−418.

Hipler, K., Priestle, J., Rahuel, J., & Grütter, M. G. (1992) *FEBS Lett. 309*, 139−145.

Hyberts, S. G., Goldberg, M. S., Havel, T. F., & Wagner, G. (1992) *Protein Sci. 1*, 736−751.

Karplus, M. (1986) *Methods Enzymol. 131*, 283−307.

Krezel, A. M., Darba, P., Robertson, A. D., Fejzo, J., Macura, S., & Markely, J. L. (1994) *J. Mol. Biol. 242*, 203−214.

Krishnamoorthi, R., Gong, Y., & Richardson, M. (1990) *FEBS Lett. 273*, 163−167.

Krishnamoorthi, R., Lin, C. S., & VanderVelde, D. (1992) *Biochemistry 31*, 4965−4969.

Laskowski, M., Jr., & Kato, I. (1980) *Annu. Rev. Biochem. 49*, 593−626.

McPhalen, C. A., & James, M. N. G. (1987) *Biochemistry 26*, 261−269.

Mueller, L. (1987) *J. Magn. Reson. 72*, 191−196.

Musil, D., Bode, W., Huber, R., Laskowski, M., Jr., Lin, T.-Y., & Ardelt, W. (1991) *J. Mol. Biol. 220*, 739−755.

Neurath, H. (1984) *Science 224*, 350−357.

Nilges, M., Clore, G. M., & Gronenborn, A. M. (1988) *FEBS Lett. 229*, 317−324.

Otlewski, J., & Zbyryt, T. (1994) *Biochemistry 33*, 200−207.

Papamokos, E., Weber, E., Bode, W., Empie, H. W., Kato, I., & Laskowski, M., Jr. (1982) *J. Mol. Biol. 158*, 515−537.

Peng, J. W., & Wagner, G. (1992) *Biochemistry 31*, 8571−8586.

Perkins, S. J., Smith, K. F., Nealis, A. S., Haris, P. I., Chapman, D., Bauer, C. J., & Harrison, R. A. (1992) *J. Mol. Biol. 228*, 1235−1254.

Rance, M., Sørensen, O. W., Bodenhausen, G., Wagner, G., Ernst, R. R., & Wüthrich, R. (1983) *Biochem. Biophys. Res. Commun. 117*, 479−485.

Shaw, G. L., Davis, B., Keeler, J., & Fersht, A. R. (1995) *Biochemistry 34*, 2225−2233.

Stryer, L. (1988) *Biochemistry*, p 189, 3rd ed., Freeman and Co., New York.

Wagner, G., Braun, W., Havel, T. F., Schaumann, T., Gō, N., & Wüthrich, K. (1987) *J. Mol. Biol. 196*, 611−639.

Walkenhorst, W. F., Krezel, A. M., Rhyu, G. I., & Markley, J. L. (1994) *J. Mol. Biol. 242*, 215−230.

Weber, E., Papamokos, E., Bode, W., Huber, R., Kato, I., & Laskowski, M., Jr. (1981) *J. Mol. Biol. 149*, 109−123.

Wen, L., Kim, S. S., Tinn, T. T., Huang, J. K., Krishnamoorthi, R., Gong, Y., Lwin, N. Y., & Kyin, S. (1993) *Protein Express. Purif. 4*, 215−222.

Wieczorek, M., Otlewski, J., Cook, J., Parks, K., Leluk, J., Wilimowska-pelc, A., Polanowski, A., Wilusz, T., & Laskowski, M., Jr. (1985) *Biochem. Biophys. Res. Commun. 126*, 646−652.

Wüthrich, K. (1986) *NMR of Protein and Nucleic Acids*, J. Wiley and Sons, New York.

BI951304E